Geometric and electronic properties of $Sc_2C_2@C_{84}$

2006 J. Phys.: Condens. Matter 18 7115

(http://iopscience.iop.org/0953-8984/18/31/006)

INSTITUTE OF PHYSICS PUBLISHING JOURNAL OF PHYSICS: CONDENSED MATTER

J. Phys.: Condens. Matter **18** (2006) 7115–7122 doi:10.1088/0953-8984/18/31/006

Geometric and electronic properties of $Sc_2C_2@C_{84}$

Haiping Wu, Kaiming Deng[1], Gongli Lu, Yongbo Yuan, Jinlong Yang and Xin Wang

Department of Applied Physics, Nanjing University of Science and Technology, Nanjing, Jiangsu 210094, People's Republic of China
and
Laboratory of Bond Selective Chemistry, University of Science and Technology of China, Hefei, Anhui 230026, People's Republic of China

E-mail: kmdeng@mail.njust.edu.cn

Received 10 February 2006, in final form 23 June 2006
Published 21 July 2006
Online at stacks.iop.org/JPhysCM/18/7115

Abstract

The geometric and electronic properties of metal–carbon encaged fullerenes $Sc_2C_2@C_{84}$ have been studied using the density functional theory at the Becke exchange gradient correction and the Perdew–Wang correlation gradient correction function level with the double numerical atomic orbitals basis sets augmented by polarization functions. The Sc_2C_2 cluster was found to be stable in C_{84} cage, while the cage expands slightly. The Sc_2C_2 cluster can rotate freely in the cage around the Sc–Sc axis which is coincident with the vertical principal axis of the cage. As the Sc_2C_2 cluster is encaged, the degeneracy of energy splits, and the HOMO–LUMO energy gap becomes smaller than that of the pure C_{84}, which suggests that $Sc_2C_2@C_{84}$ has higher reactivity than C_{84}. Based on our calculated results, the electronic structure of $Sc_2C_2@C_{84}$ might be formally described as $(Sc_2C_2)^{+1}@(C_{84})^{-1}$ due to the charge transferring from the Sc_2C_2 cluster to C_{84} cage.

1. Introduction

Endohedral fullerenes, as derivatives of fullerenes, have attracted a lot of attention since fullerenes were at their infancy [1, 2]. Fullerenes have a unique type of inner empty space with an unusual cage-like structure that it is possible to put metal atoms [3, 4], metal clusters [5], metal nitrides [6], nitrogen atoms [7–9] and noble gas atoms [10–12] into the cages, to form endohedral fullerenes. These new series of materials with novel physical and chemical properties are very important for their potential application as new types of superconductors, organic ferromagnets, nonlinear optical materials, functional molecular devices, magnetic resonance imaging agents, and biological trace agent [3, 4]. Recently, experimental evidence

[1] Author to whom any correspondence should be addressed.

that carbides can be encapsulated inside fullerenes to form the scandium carbide endohedral fullerene $Sc_2C_2@C_{84}$ was reported [13]. This is the first endohedral metal–carbon-cluster fullerene. The relative yield of $Sc_2C_2@C_{84}$ is about 2% of that of C_{60}, which is lower than those of the most abundant discandium metallofullerenes $Sc_2@C_{84}$ and $Sc_2@C_{82}$, but higher than those of all other metallofullerenes. The abundant product makes it possible to study its intriguing geometric and electronic structure experimentally. Both nuclear magnetic resonance (NMR) and synchrotron x-ray structural analysis [13] revealed that the molecular structure of $Sc_2C_2@C_{84}$ has D_{2d} (no. 23) symmetry and the Sc_2C_2 is inside the C_{84} cage. However, to the best of our knowledge, there is so far no theoretical study on its novel properties.

In this paper, we report a first-principles study of $Sc_2C_2@C_{84}$ to explore its structural and electronic properties. We describe our computational method in section 2 and present our results and discussions in section 3. Finally, a summary is given in section 4.

2. Computational method

Our calculations are based on the density functional theory (DFT). The Becke [14] exchange gradient correction and the Perdew–Wang [15] correlation gradient correction function (BLYP) together with the DNP basis functions are chosen. The DNP basis functions are the double numerical atomic orbitals augmented by polarization functions, i.e., functions with angular momentum one higher than that of the highest occupied orbital in the free atom. The electronic structure is obtained by solving the Kohn–Sham [16, 17] equations self-consistently using the spin unrestricted scheme. The inner core electrons are frozen to simplify the computation without significantly sacrificing the accuracy [18]. The medium grid mesh points within the DMOL [19] package are employed for the matrix integrations. Self-consistent field procedures are carried out with a convergence criterion of 10^{-6} a.u. on the energy and electron density. Geometry optimizations are performed using the Broyden–Fletcher–Goldfarb–Shanno (BFGS) algorithm [20] with a convergence criterion of 10^{-3} a.u. on the gradient, 10^{-3} a.u. on the displacement and 10^{-5} a.u. on the energy. The uncertainty of the relative total energy for different isomers in our scheme is within 0.001 eV.

3. Results and discussion

3.1. Stability and geometry of $Sc_2C_2@C_{84}$

For the C_{84} fullerene, there are 24 isomers satisfying the so-called isolated pentagon rule [21], and they are denoted as isomers **1**–**24**. The NMR study [22] demonstrates that only isomer **22** (D_2) and isomer **23** (D_{2d}) are abundantly produced as a 2:1 mixture [22] and these two isomers are very close in energy and much more stable than the remaining 22 isomers. When the planar cluster Sc_2C_2 is encapsulated into the carbon cage to form $Sc_2C_2@C_{84}$, the NMR spectrum only shows D_{2d} characteristics, so we perform geometry optimization of C_{84} with D_{2d} symmetry as the start point. Our optimized C–C bond lengths range from 1.374 to 1.477 Å with the average 1.439 Å, in good agreement with the results obtained by Sun *et al* [23], i.e. from 1.367 to 1.471 Å with the average 1.432 Å at B3LYP level. These results indicate that our computational scheme is suitable for studying the fullerenes.

The D_{2d}–C_{84} cage has three C_2 axes, and we call them axis **1**, axis **2** and axis **3** respectively, as shown in figure 1. Each of them bisects the double bonds at the fusion of two hexagonal rings, and they are orthogonal to each other. Axis **1** is the vertical one, while axis **2** and axis **3** are on the horizontal plane. There are two symmetrical planes, which are orthogonal to each other and bisect axis **2** and axis **3**. Their intersecting line is coincident with axis **1**. Because

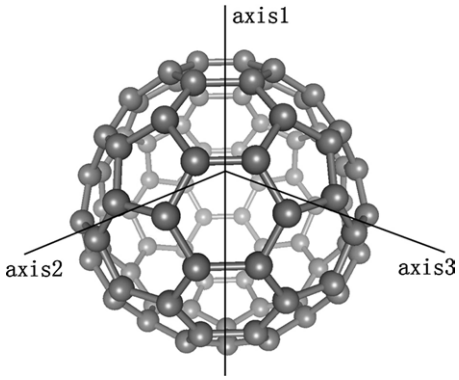

Figure 1. C_{84} with its three principal axes.

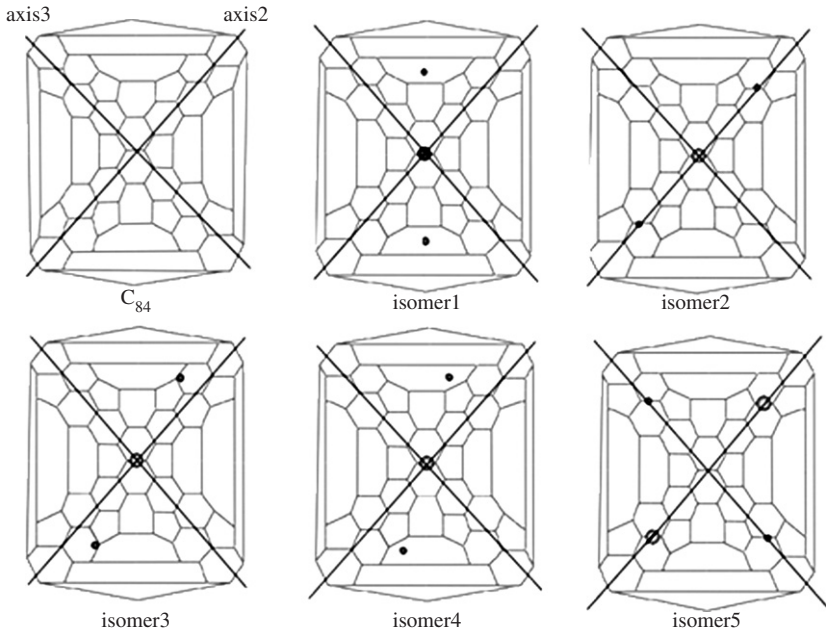

Figure 2. The Schlegel-like diagrams for C_{84} and five $Sc_2C_2@C_{84}$ isomers.

of the D_{2d} symmetry, if a planar molecule, like Sc_2C_2 with D_{2h} symmetry, rotates around axis **1** in the cage, the different orientations that should be considered for the planar molecule are only within 45° of its angular displacement. So five geometries of $Sc_2C_2@C_{84}$ were chosen to be optimized with different orientations of the planar Sc_2C_2, which are called isomers **1**–**5**, respectively. Figure 2 gives the Schlegel-like diagrams for C_{84} and five $Sc_2C_2@C_{84}$ isomers, in which small balls stand for carbon atoms, while big balls stand for Sc atoms. The Sc–Sc axes of isomers **1**–**4** are on axis **1** and their C–C axes are on the horizontal plane. The C–C axis of isomer **1** is in one of the symmetric planes of the C_{84} cage and makes 45° with axis **2**, while the C–C axis of isomer **2** is on axis **2**. The C–C axis of isomer **3** and that of isomer **4** are at 15° and 30° from axis **2**, respectively. For isomer **5**, the Sc–Sc axis is on axis **2** while the C–C axis is on axis **3**.

Table 1. Binding energy (BE), HOMO, LUMO, and energy gap for C_{84}, free Sc_2C_2 and the five different isomers of $Sc_2C_2@C_{84}$, in eV.

	C_{84}	Sc_2C_2	Isomer **1**	Isomer **2**	Isomer **3**	Isomer **4**	Isomer **5**
BE	598.42	15.70	619.20	619.17	619.19	619.17	618.28
LUMO	−4.62	−2.56	−4.44	−4.45	−4.45	−4.46	−4.77
HOMO	−5.71	−2.64	−5.24	−5.25	−5.26	−5.27	−4.96
Gap	1.09	0.08	0.80	0.80	0.81	0.81	0.19

Table 1 presents the binding energies, the energies of the highest occupied molecular orbital (HOMO) and the lowest unoccupied molecular orbital (LUMO) together with the energy difference (Gap) between them for the optimized D_{2d}–C_{84}, free Sc_2C_2 cluster and the $Sc_2C_2@C_{84}$ isomers. The most striking result found from the table is that the first four isomers almost have the same binding energies and their differences are no more than 0.03 eV, implying that they are quasi-isoenergetic, while isomer **1** has the highest binding energy among them. What is more interesting is that these four isomers have nearly the same HOMO–LUMO energy gap. If there is a consensus that the relative stability of different isomers of a molecule mainly depends on the binding energy as well as the energy gap between the HOMO and the LUMO, then we can come to the conclusion that these four isomers have almost the same stability, which means that if we rotate the planar cluster Sc_2C_2 around axis **1** there is no energy barrier. This result can be used to explain the NMR phenomenon that the NMR spectrum of $Sc_2C_2@C_{84}$ consists of 12 distinct lines (with intensities 10×8, 1×4, 1×2), of which 11 can be assigned to the D_{2d}–C_{84} cage, and the one line with intensity 1×2 to Sc_2C_2. This last line resulting from Sc_2C_2 suggests that the rotation of Sc_2C_2 around axis **1** is free; this yields a time-averaged electronic environment that preserves the overall D_{2d} symmetry. Both the binding energy and energy gap of isomer **5** are smaller than those of isomer **1** by 0.92 and 0.61 eV, respectively, indicating that it is less stable than isomer **1**. Thus, the planar Sc_2C_2 cluster can only rotate freely about the Sc–Sc axis, coincident with axis **1**, but is not completely free to rotate in the cage. Another thing worth noticing is that the binding energies of the first four $Sc_2C_2@C_{84}$ isomers are about 5.0 eV higher than the sum of those of Sc_2C_2 and C_{84}, implying that encapsulating Sc_2C_2 into the C_{84} cage is a exothermic and stabilizing process.

The geometric properties of isomer **1** are compared with other relevant results. It is found that the theoretical bond lengths of $Sc_2C_2@C_{84}$ are, by and large, consistent with experimental ones. The C–C bond lengths of the $Sc_2C_2@C_{84}$ cage range from 1.388 to 1.484 Å with the average 1.442 Å, a little larger than their counterparts of D_{2d}–C_{84} that range from 1.374 to 1.477 Å with the average 1.439 Å. This means that the $Sc_2C_2@C_{84}$ cage expands a little after Sc_2C_2 is encaged within it. However, the two mutually orthogonal C–C bonds over the two the Sc atoms in the cage experience the most conspicuous change, i.e., from 1.38 to 1.45 Å, so the four carbon atoms in the polar region are popped out. From table 2, it can be found that the Sc–Sc distance elongates distinctly while the C–C distance shrinks a lot compared with free Sc_2C_2, so Sc_2C_2 becomes slim after having been put into the cage. Besides these, the distance between Sc and the carbon atoms of the cage becomes shorter in the $Sc_2C_2@C_{84}$ cage compared with that in $Sc_2@C_{84}$ cage. Therefore we can get the scenario that the two carbons of Sc_2C_2 in the cage have strong bonding, and the Sc has bonding not only with the carbons of Sc_2C_2 but also with the carbons of the cage nearest it. This conclusion can also be obtained from the map of charge density on the Sc_2C_2 plane in isomer **1**.

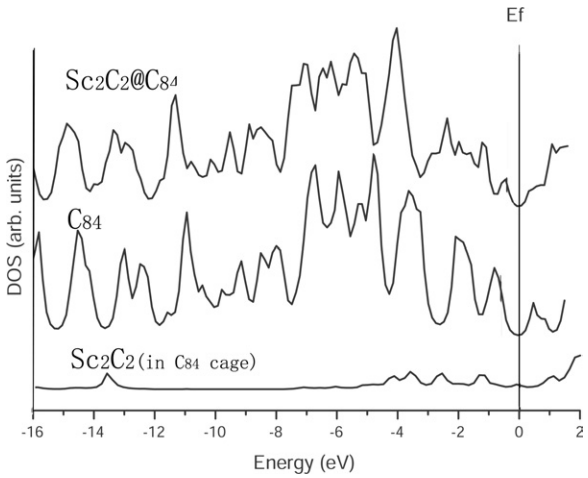

Figure 3. TDOS for isomer **1** of $Sc_2C_2@C_{84}$ and D_{2d}–C_{84}, and partial DOS for Sc_2C_2 in $Sc_2C_2@C_{84}$.

Table 2. Bond lengths (in Å) of $Sc_2C_2@C_{84}$, in which C(1)and C(2) are the two carbon atoms in the planar cluster of Sc_2C_2, while C(3) is the cage carbon atom, which has the nearest distance to Sc atom.

Cluster	Sc–Sc	Sc–C(1, 2)	C(1)–C(2)	Sc–C(3)	Source
$Sc_2C_2@C_{84}$	4.41	2.29	1.27	2.26	This work
$Sc_2C_2@C_{84}$	4.29(2)	2.26(3)	1.42(6)		Exp. [24]
Sc_2C_2	3.95	2.08	1.37		This work
$Sc_2@C_{84}$	4.03			2.36	Theory [26]
$Sc_2@C_{84}$	3.9			2.4	Exp. [5]

3.2. Electronic structure of $Sc_2C_2@C_{84}$

Here we take isomer **1** as an example to discuss the electronic structure of $Sc_2C_2@C_{84}$ because it is the ground state of the isomers. Figure 3 presents the total density of state (TDOS) for $Sc_2C_2@C_{84}$ and D_{2d}–C_{84}, as well as the partial density of state (PDOS) for Sc_2C_2 in $Sc_2C_2@C_{84}$. They were obtained by a Lorentzian extension of the discrete energy levels and a summation over them. The broadening width parameter was chosen to be 0.15 eV and the Fermi energy (Ef) is defined as the energy position of midpoint between HOMO and LUMO. It can be seen from the figure that the TDOS of $Sc_2C_2@C_{84}$, compared with the TDOS of the pure C_{84}, changes mainly in the region from −5.0 to 0.0 eV, while the region far from the zero still retains the character of the pure C_{84} except for a little relative displacement because the Fermi level of $Sc_2C_2@C_{84}$ is about 0.34 eV higher than that of the C_{84} cage. The TDOS for $Sc_2C_2@C_{84}$ has several peaks in the region from −5.0 to 0.0 eV, while that of C_{84} has only three peaks. This difference derives from interaction between Sc_2C_2 and C_{84} cage, which is in accordance with the evidence that there are many peaks of the PDOS for Sc_2C_2 from −5.0 to 0.0 eV.

Figure 4 shows the energy levels of free Sc_2C_2, D_{2d}–C_{84} and $Sc_2C_2@C_{84}$. The molecular orbitals whose energies agree with each other within a difference of 0.05 eV are regarded as degenerate. The length of the horizontal bar shows the orbital degeneracy, while the real line shows the occupied orbitals and the broken line shows the unoccupied orbitals. Three

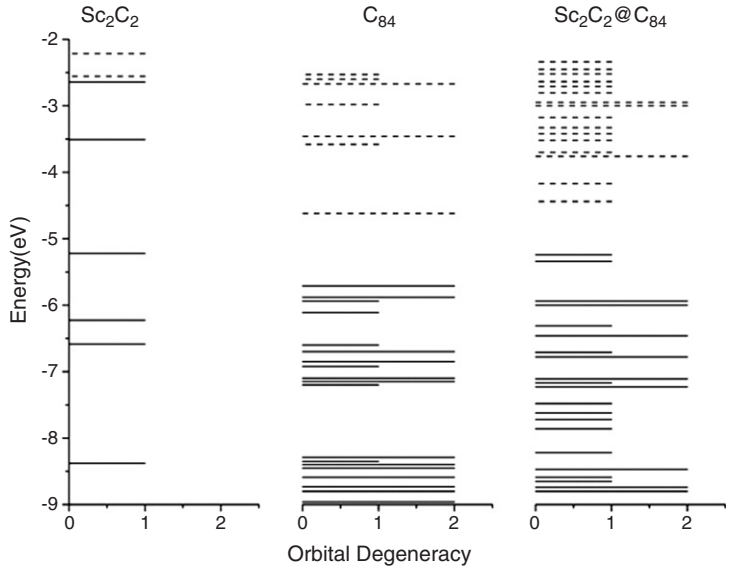

Figure 4. The energy level map of Sc_2C_2, C_{84}, and isomer **1** of $Sc_2C_2@C_{84}$.

energy blocks in C_{84} but many dense energy lines in $Sc_2C_2@C_{84}$ can be seen in the figure, corresponding to the three peaks in C_{84} TDOS, and several dense peaks in the $Sc_2C_2@C_{84}$ TDOS near the zero energy respectively, indicating the orbital mixture between Sc_2C_2 and carbon atoms of the cage.

The charge transformation of the atoms was obtained from a Mulliken population analysis. Our calculation shows that each Sc atom loses $0.79e$, and each C atom of Sc_2C_2 gets $0.31e$, which means that only $0.96e$ is transferred from Sc_2C_2 to the cage. It is well known that a scandium atom takes a trivalent chemical state upon forming compounds. Both our result and the estimation of the experiment show that scandium atoms in the C_{84} cage take an intermediate valency between the metal (Sc^0) and the oxide (Sc^{3+}), which has been found in the fullerene $Sc_2@C_{84}$ [25]. We also performed a single point calculation of $Sc_2C_2@C_{84}$ at the BP level, based on the optimized geometry in order to check whether the number of transferred charges calculated by us is precise. The result is $0.8e$ transferred from Sc_2C_2 to the cage, which agrees well with the result obtained at BLYP level. So based on our calculation, the formal electronic structure of $Sc_2C_2@C_{84}$ can be described as $(Sc_2C_2)^{+1}@(C_{84})^{-1}$, instead of $(Sc_2C_2)^{+2}@(C_{84})^{-2}$ given by Chun-Ru *et al* [13].

The map of charge density difference of $Sc_2C_2@C_{84}$ on the plane of the Sc_2C_2 atoms is given in figure 5. From this map, we find each of the two Sc atoms forms weak bonds with the nearest two hexagon rings of the cage. Furthermore, one strong σ bond between two C atoms and four Sc–C bonds in the Sc_2C_2 plane can be seen. This indicates that the Sc_2C_2 cluster exists as a whole in the cage.

Finally, we calculated the vertical ionization potentials (IPs) and the vertical electron affinities (EAs) of C_{84} and the four most stable $Sc_2C_2@C_{84}$ isomers. The vertical IP is the energy difference between the positively charged and neutral clusters at the equilibrium geometry of the neutral cluster. The vertical EA is evaluated by adding one electron to the neutral cluster in its equilibrium geometry and taking the difference between their total energies. The calculated IP and EA of C_{84} are 7.07 and 3.23 eV, while the IP and EA of isomer **1** of $Sc_2C_2@C_{84}$ are 5.82 and 3.06 eV. The same conclusion that $Sc_2C_2@C_{84}$ has higher chemical

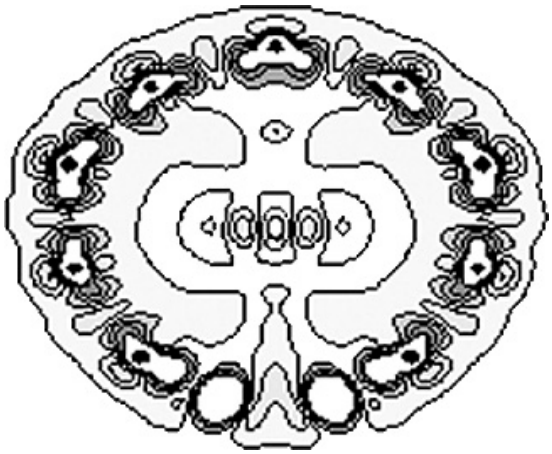

Figure 5. The map of charge density of $@C_{84}$ on the plane of the Sc_2C_2 atoms.

reactivity than C_{84} as above can be obtained. We expect further experimental measurements to confirm them.

4. Summary

The binding energy of the most stable geometry of $Sc_2C_2@C_{84}$ is higher than the sum of the binding energy of Sc_2C_2 and that of C_{84}, indicating that metal–carbon Sc_2C_2 can be encapsulated in the C_{84} cage stably. The C_{84} cage expands very slightly after Sc_2C_2 is encaged. The C–C bonds lengths of the C_{84} cage changed slightly, but the two C–C bonds nearest to the two Sc atoms at the fusion of two hexagonal rings pop out obviously. The binding energy and the HOMO–LUMO energy gaps of the different isomers whose Sc–Sc axes are on the principal axis **1** are almost the same values, and much lower than those of the other isomer whose Sc–Sc axis is off axis **1**, indicating that the Sc_2C_2 could rotate around axis **1** in the C_{84} cage, but is not completely free to rotate in the cage. The electronic structure of $Sc_2C_2@C_{84}$ is formally described as $(Sc_2C_2)^{+1}@(C_{80})^{-1}$ as a result of the charge that is transferred from the Sc_2C_2 cluster to the C_{84} cage. Both the IPs and the EAs of the most stable $Sc_2C_2@C_{84}$ isomers whose Sc–Sc axes are on the main rotational axis **1** are smaller than those of the pure C_{84} cage, which shows that these structures of $Sc_2C_2@C_{84}$ are more active than the pure C_{84}.

Acknowledgments

This work was partially supported by the National Natural Science Foundation of China under Grant No 10174039, and the Jiangsu Natural Science Foundation under Grant No BK2002099.

References

[1] Kroto H W *et al* 1985 *Nature* **318** 162
[2] Heath J R *et al* 1985 *J. Am. Chem. Soc.* **107** 779
[3] Liu S and Sun S 2000 *J. Organmet. Chem.* **599** 74
[4] Shinohara H 2000 *Rep. Prog. Phys.* **63** 843
[5] Takata M *et al* 1999 *Phys. Rev. Lett.* **83** 2214
[6] Stevenson S *et al* 1999 *Nature* **401** 55

[7] Almeida Murphy T *et al* 1996 *Phys. Rev. Lett.* **77** 1075
[8] Knapp C *et al* 1997 *Chem. Phys. Lett.* **272** 433
[9] Mauser H *et al* 1997 *Angew. Chem. Int. Edn Engl.* **36** 2835
[10] Yamamoto K *et al* 1999 *J. Am. Chem. Soc.* **121** 1591
[11] Weiske T *et al* 1991 *Angew. Chem.* **103** 898
Weiske T *et al* 1991 *Angew. Chem. Int. Edn Engl.* **30** 884
[12] Saunders M *et al* 1996 *Science* **271** 1693
[13] Wang C-R *et al* 2001 *Angew. Chem. Int. Edn* **40** 397
[14] Becke A D 1988 *J. Chem. Phys.* **88** 1053
[15] Perdew J P and Wang Y 1992 *Phys. Rev.* B **45** 13244
[16] Hohenberg P and Kohn W 1964 *Phys. Rev.* **136** B864
[17] Kohn W and Sham L J 1965 *Phys. Rev.* A **140** 1133
[18] Baerends E J, Ellis D E and Ros P 1973 *Chem. Phys.* **2** 41
[19] DMOL v960 Biosym Technologies San Diego, CA 1996
[20] Fletcher R 1980 *Practical Methods of Optimization* vol 1 (New York: Wiley)
[21] Fowler P W and Manolopoulos D E 1995 *An Atlas of Fullerenes* (Oxford: Oxford University Press)
[22] Kikuchi K *et al* 1992 *Nature* **357** 142
[23] Sun G and Kertesz M 2001 *J. Phys. Chem.* A **105** 5212–20
[24] Wang C Z, Zhang B L and Ho K M 1992 *Phys. Rev. Lett.* **69** 69
[25] Takahashi T, Ito A, Inakuma M and Shinohara H 1995 *Phys. Rev.* B **52** 13812
[26] Nagase S and Kobayashi K 1994 *Chem. Phys. Lett.* **231** 319